

# Terahertz microdisk based on 3D-printed $\text{Al}_2\text{O}_3$ for temperature sensing

Zhibo Hou

Wuhan National Laboratory for  
Optoelectronics and School of Optical  
and Electronic Information  
Huazhong University of Science and  
Technology  
Wuhan 430074, China  
zbhou@hust.edu.cn

Liao Chen

Wuhan National Laboratory for  
Optoelectronics and School of Optical  
and Electronic Information  
Huazhong University of Science and  
Technology  
Wuhan 430074, China  
liaochenchina@hust.edu.cn

Shixing Yuan

Wuhan National Laboratory for  
Optoelectronics and School of Optical  
and Electronic Information  
Huazhong University of Science and  
Technology  
Wuhan 430074, China  
shxyuan@hust.edu.cn

Jiamin Wu

School of Materials Science and  
Engineering and State Key Laboratory  
of Material Processing and Die &  
Mould Technology  
Huazhong University of Science and  
Technology  
Wuhan 430074, China  
jiaminwu@hust.edu.cn

Xiaojun Wu

School of Electronic and Information  
Engineering  
Beihang University  
Beijing 100191, China  
xiaojunwu@buaa.edu.cn

Xinliang Zhang\*

Wuhan National Laboratory for  
Optoelectronics and School of Optical  
and Electronic Information  
Huazhong University of Science and  
Technology  
Wuhan 430074, China  
Corresponding author:  
xlzhang@mail.hust.edu.cn

**Abstract**—We propose and fabricate a microdisk using  $\text{Al}_2\text{O}_3$  based on 3D-printed technology. The Q factor reaches 267 and the temperature sensing sensitivity reaches  $32.3 \pm 0.8 \text{ MHz}/^\circ\text{C}$ .

**Keywords**—Terahertz, Microdisk, Whispering Gallery Mode (WGM), 3D-printed  $\text{Al}_2\text{O}_3$ , Sensing

## I. INTRODUCTION

Terahertz (THz) technology has made tremendous progress in the last twenty years and has great potential in sensing [1]. THz resonators have been applied for refractive index sensing [2]. THz resonators include metasurfaces [3], whispering gallery mode resonators (WGMRs) [4], F-P cavities [5], and photonic crystals [6]. The fabrication is commonly based on silicon via CMOS-compatible technology, which possesses the ability to manufacture delicate plane structures. 3D structures have been achieved by multi-step etching [7], but the complex operation is the limitation. Therefore, developing convenient and concise fabrication of 3D structure devices is necessary.

3D-printed technology is a competitive way for fast prototyping and fabrication [8]. Based on different materials, 3D printing has carried out work in wavefront control [9], and other fields. THz 3D-printed technology mainly focuses on the characterization of the waveguide, while the design and experimental measurement of WGMRs is rarely mentioned. Among these, Ceramics  $\text{Al}_2\text{O}_3$  has a higher refractive index and shows a low absorption coefficient at THz frequencies [10]. Therefore, 3D-printed  $\text{Al}_2\text{O}_3$  may provide an effective alternative technology for integrated THz resonators.

In this work, a microdisk based on the 3D-printed  $\text{Al}_2\text{O}_3$  technology is manufactured and used for THz sensing. We experimentally observe the WGMs and their Q factors which can reach 267. The 3D-printed  $\text{Al}_2\text{O}_3$  microdisk is applied in temperature sensing, and the achieved sensitivity is  $32.3 \pm 0.8 \text{ MHz}/^\circ\text{C}$ .

## II. PRINCIPLE AND EXPERIMENTAL SETUP

Limited by the accuracy of 3D printing, the traditional coupling structure based on evanescent field coupling is inappropriate. Referring to the principles of the end-fire

injection disk [11], the waveguides are designed to directly connect with the microdisk. As shown in Fig. 1a, two straight waveguides are used as the input and output of THz waves, and the microdisk is used as the resonator.

The size of the microdisk is mainly limited by the printing precision. To ensure the strength and stability of the structures during the sinter, the thickness  $h$  of the device is designed as  $600 \mu\text{m}$ , the width  $w$  of the input and output waveguide is  $1 \text{ mm}$ , and the radius  $r$  of the microdisk is  $4.4 \text{ mm}$ .

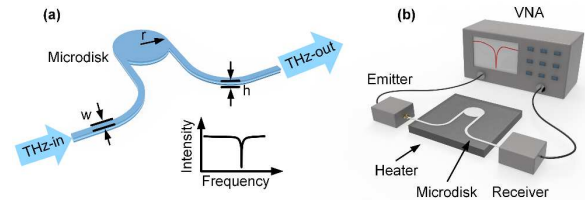


Fig. 1. (a) The structure diagram of the microdisk. The inset illustrates the transmission spectrum of the microdisk. (b) The experimental setup. The heater under the microdisk is applied to adjust the temperature and the spectrum is acquired from the vector network analyzers (VNA) (Ceyear 3649B).

The manufacture is based on Stereolithography (SL). The measurement is performed on the vector network analyzers (VNA) (Ceyear 3649B). The input and output waveguides are aligned to the emitter and receiver of the VNA.

As mentioned in Fig. 2, the simulated results imply the microdisk supports the WGMs. The insets demonstrate the electric field distributions of the microdisk at  $475.8 \text{ GHz}$  and  $480.3 \text{ GHz}$ . The electric field mainly lies in the microdisk when the frequency is  $475.8 \text{ GHz}$ , however, the THz waves mainly export in the output at  $480.3 \text{ GHz}$ .

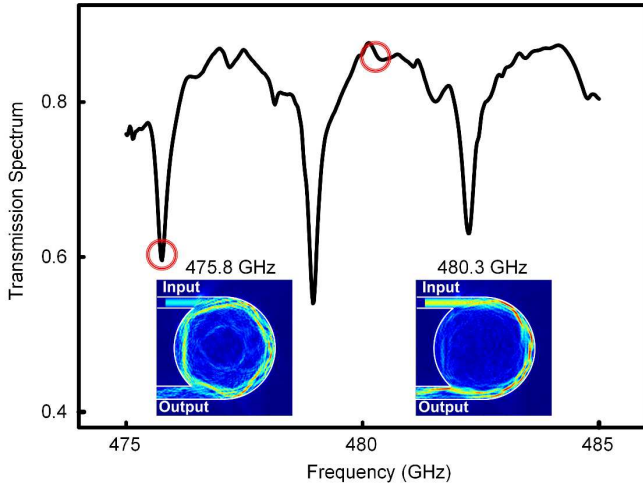


Fig. 2. The simulated transmission spectrum and electric field distributions of the designed microdisk.

### III. RESULTS AND DISCUSSION

To demonstrate the temperature sensing performance, THz waves from the VNA are coupled into the microdisk. The intensity transmission spectra of the microdisk are obtained in the target frequency band by frequency scanning. The microdisk is placed on the heater with controlled temperatures ranging from 20 °C to 75 °C.

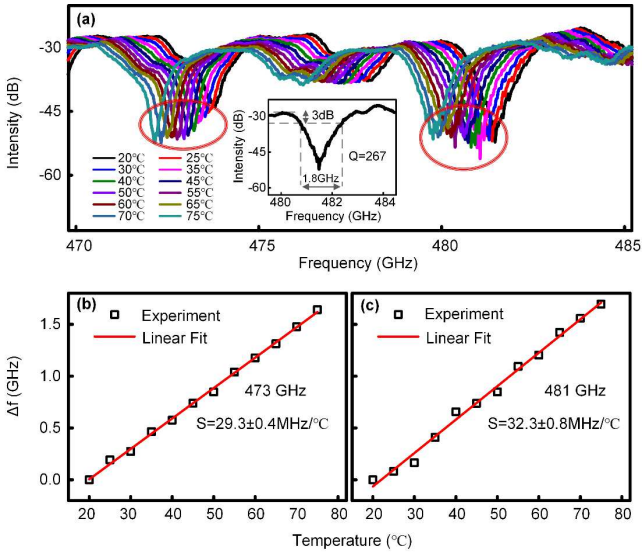


Fig. 3. (a) The transmission spectra of the microdisk at different temperatures. The inset demonstrates the Q factor of the microdisk. (b) (c) The frequency shifts of the microdisk at different temperatures for the modes around 473 GHz and 481 GHz.

As depicted in Fig. 3a, the resonance dips demonstrate that the microdisk supports the WGMs, and the refractive index of the  $\text{Al}_2\text{O}_3$  increases with the augment of temperature, therefore the resonant frequency decreases. The inset illustrates the resonance mode around 481.5 GHz at 20 °C, which illustrates the full width at half-maximum (FWHM) is 1.8 GHz and the Q factor is 267. The frequency shifts of the resonance dip are acquired and depicted in Fig. 3b and Fig. 3c. The black squares demonstrate the experimental results, and the red line is the linear fit of the experimental results. The slopes of the red lines imply the sensing sensitivity. As illustrated in Fig. 3b, the frequency shift is approximately

linear with the temperature, and the sensitivity of the sensor is  $29.3 \pm 0.4 \text{ MHz/}^\circ\text{C}$  for the mode around 473 GHz. To compare the results, another mode around 481 GHz is also performed for temperature sensing. The results are depicted in Fig. 3c and the sensitivity is  $32.3 \pm 0.8 \text{ MHz/}^\circ\text{C}$ . Noteworthy, the sensitivities are different for different modes. We postulate that the mode around 481 GHz possesses a larger overlapping area with the microdisk, therefore, experiencing a larger change in the effective refractive index of the THz waves.

### IV. CONCLUSIONS

In this work, we design and experimentally perform the microdisk based on the 3D-printed  $\text{Al}_2\text{O}_3$  technology. The microdisk supports the WGMs successfully. The Q factor of the microdisk reaches 267. The microdisk is applied in the temperature sensing. The experimental results demonstrated a linear relationship between the frequency shifts and the temperature and the sensitivity reaches  $32.3 \pm 0.8 \text{ MHz/}^\circ\text{C}$ . Based on the low-cost, fast monolithic fabrication of complex structures for small-volume production, the printed  $\text{Al}_2\text{O}_3$  microdisk will provide a great convenience for THz sensing applications.

### ACKNOWLEDGMENT

This work is supported by grants from the National Natural Science Foundation of China (NSFC) (Grants No. 61927817, 62005090, 61735006, 61631166003, 61675081, and 61505060).

### REFERENCES

- [1] R. Singh *et al.*, "Ultrasensitive terahertz sensing with high-Q Fano resonances in metasurfaces," *Appl. Phys. Lett.*, vol. 105, p. 171101, 2014.
- [2] Z. Hou *et al.*, "Crystalline hydrate dehydration sensing based on integrated terahertz whispering gallery mode resonators," *Sensors*, vol. 22, p. 9116, 2022.
- [3] S. W. Jun and Y. H. Ahn, "Terahertz thermal curve analysis for label-free identification of pathogens," *Nat. Commun.*, vol. 13, p. 3470, 2022.
- [4] S. Yuan *et al.*, "On-chip terahertz isolator with ultrahigh isolation ratios," *Nat. Commun.*, vol. 12, p. 5570, 2021.
- [5] R. Damari *et al.*, "Strong coupling of collective intermolecular vibrations in organic materials at terahertz frequencies," *Nat. Commun.*, vol. 10, p. 3248, 2019.
- [6] K. Okamoto *et al.*, "Terahertz sensor using photonic crystal cavity and resonant tunneling diodes," *J infrared millim te*, vol. 38, pp. 1085-1097, 2017.
- [7] M. Aamer *et al.*, "CMOS compatible silicon-on-insulator polarization rotator based on symmetry breaking of the waveguide cross section," *IEEE Photonics Technol. Lett.*, vol. 24, pp. 2031-2034, 2012.
- [8] J. Ornik, M. Sakaki, M. Koch, J. C. Balzer, and N. Benson, "3D printed  $\text{Al}_2\text{O}_3$  for terahertz technology," *IEEE Access*, vol. 9, pp. 5986-5993, 2021.
- [9] W. D. Furlan *et al.*, "3D printed diffractive terahertz lenses," *Opt. Lett.*, vol. 41, pp. 1748-1751, 2016.
- [10] K. Z. Rajab *et al.*, "Broadband dielectric characterization of aluminum oxide ( $\text{Al}_2\text{O}_3$ )," *J. Microelectron. Electron. Packag.*, vol. 5, pp. 2-7, 2008.
- [11] S. Liu *et al.*, "End-fire injection of guided light into optical microcavity," *Appl. Phys. B*, vol. 120, pp. 255-260, 2015.